

# ANALYSIS OF MULTIPACTING IN COAXIAL LINES

E. Somersalo, P. Ylä-Oijala, Rolf Nevanlinna Institute, University of Helsinki, PO Box 26, 00014  
University of Helsinki, Finland

D. Proch, DESY, Notkestrasse 85, 2000 Hamburg 52, Germany

## Abstract

Multipacting can cause breakdown in high power rf components like couplers, windows, etc. This phenomenon starts if certain resonant conditions for electron trajectories are fulfilled and if the impacted surface has a secondary yield larger than one. A general cure against multipacting is to avoid the resonant conditions. Therefore we investigated the dynamics of the electron trajectories in order to find rules for these resonances and thus suppress multipacting by appropriate design. We developed a new code which combines standard trajectory calculations with advanced searching and analyzing methods for multipacting resonances. As a first step, coaxial power lines are investigated. We characterize multipacting behavior in straight and tapered lines and give scaling laws with respect to dimension, frequency and impedance. The calculations are compared with experimental observations.

## I. INTRODUCTION

This paper gives a brief description of a code developed for analyzing multipacting in rf cavities. The code consists of two main elements: The first step is to recognize those rf power levels in the given geometry that are able to multipact. The second step is to locate and identify the possible multipacting processes. The core of the code consists of standard trajectory calculations. The novel feature is a systematic application of ideas arising from the theory of dynamical systems.

## II. THEORETICAL BACKGROUND

Physically, the multipacting process is described as follows. An electron is emitted from the surface of an rf cavity and driven by the field. When it impacts the cavity wall, it may release one or more electrons from the surface layer of the wall, the number of the secondary electrons depending on the impact energy and the wall material characteristics. These secondary electrons are again accelerated by the field, yielding new impacts and possibly new secondary electrons. In appropriate conditions, the number of electrons may increase exponentially, leading to remarkable power losses, gassing of the surface and heating of the walls.

The following is a brief summary of the mathematical description of the process, which constitutes the background of the programs used for analyzing the multipacting processes in rf cavities.

### A. Dynamical system

Consider a void cavity  $\Omega$  with a time harmonic rf field. Denoting by  $f$  the rf frequency, the electric and magnetic fields can be written as

$$\vec{E}(x, t) = \vec{E}(x) \sin 2\pi ft, \quad \vec{B}(x, t) = \vec{B}(x) \cos 2\pi ft,$$

where  $\vec{E}(x)$  and  $\vec{H}(x)$  are the spatial amplitudes of the fields. Let  $\varphi$  denote the phase angle of the field,  $0^\circ \leq \varphi < 360^\circ$ . Consider an electron being emitted at a point  $x$  of the cavity wall  $\partial\Omega$ , the field phase at the time of emission being  $\varphi$ . Assuming that the rf field map in the cavity is known, it is a straightforward matter to compute the relativistic trajectory of the electron driven by the field. Denote by  $x'$  the point where the electron hits the cavity wall for the first time. If the phase of the field at the time of the impact is denoted by  $\varphi'$ , we have a mapping

$$R : (x, \varphi) \mapsto (x', \varphi').$$

Using the notation  $X = \partial\Omega \times [0^\circ, 360^\circ]$ , the above mapping  $R$  defines a dynamical system in the phase space  $X$ : Each point  $p = (x, \varphi) \in X$  generates a discrete trajectory  $\{p, R(p), R^2(p), \dots\}$ . For each initial point  $p \in X$ , there are two possibilities: It may happen that after a finitely many impacts, the field phase is such that the electric field prevents the electron from escaping the wall. In this case, the discrete trajectory remains finite. The other possibility is that the discrete trajectory is infinite. The latter case is the geometric condition for the multipacting to occur.

Besides the geometry of the trajectories, the analysis needs to contain the secondary electron yield characteristic to the surface properties. Given an electron trajectory starting at a point  $p$ , the kinetic impact energy  $E_{\text{kin}}(p)$  can be computed. If the secondary electron yield of the cavity wall is denoted by  $\delta$ , the number of secondary electrons due to one single electron starting at  $p$  is in the average given by  $\alpha(p) = \delta(E_{\text{kin}}(p))$ . Considering the full discrete trajectory, the number of secondary electrons due to one single electron starting at  $p$  after  $n$  impacts is

$$\begin{aligned} \alpha_n(p) &= \alpha(p) + \alpha(p)\alpha(R(p)) + \dots \\ &+ \alpha(p)\alpha(R(p)) \dots \alpha(R^n(p)). \end{aligned}$$

### B. Distance function

A special case of the infinite trajectories that leads to resonant multipacting is when periodic trajectories appear. This corresponds to fixed points of the mapping, i.e.,

$$R(p) = p$$

for some  $p \in X$ , or more generally,

$$R^n(p) = p, \quad n = 1, 2, \dots$$

Physically, this corresponds to a situation where an electron trajectory hits eventually the same wall point in the same field phase where it started. This condition is fulfilled in the earlier described multipacting phenomena, and it seems to be a potentially dangerous resonant condition in general. An effective way

of searching for those points  $p$  in the phase space is to consider the distance function

$$d_n(p) = \sqrt{|x - x_n|^2 + \gamma|e^{i\varphi} - e^{i\varphi_n}|^2},$$

where  $p = (x, \varphi)$  and  $(x_n, \varphi_n) = R^n(p)$ . Here,  $\gamma$  is a scaling constant. The distance function  $d_n$  tells how far away the trajectory is after  $n$  impacts from the initial point. If  $d_n(p)$  is small for  $n$  large, the point  $p$  is likely to be prone to multipacting.

### III. COMPUTATIONS

To obtain reliable results, the rf field maps have to be known rather accurately in the cavity. In straight coaxial lines discussed below, the field map is no problem since it is analytically known. In the other cases, one has to use a numerical scheme. We have developed a suitable numerical code for computing the fields in axisymmetric geometries. The code is based on boundary integral equations, with extra care being taken for the accuracy of the computations close to the walls.

The multipacting analysis was implemented along the following lines. Given a cavity  $\Omega$  and the corresponding rf field map, we picked a large number of initial points  $p_j$  in the phase space  $X$  associated to the boundary and for each point  $p_j$  computed the discrete trajectory  $\{p_j, R(p_j), R^2(p_j), \dots\}$ . After a fixed number  $n$  of iterations of the map  $R$ , we counted those electron trajectories that were still able to multipact. This number, denoted by  $c_n$ , was computed repeatedly for different incident rf field powers. If at a given incident power no multipacting can occur and the discrete trajectories  $\{p_j, R(p_j), R^2(p_j), \dots\}$  are short, the number  $c_n$  is very small. The multipacting powers stand out clearly as having an elevated  $c_n$  value.

Having the counter function  $c_n$  computed, we plotted the distance function  $d_n(p_j)$  for those rf power values where  $c_n$  was large. The minima of  $d_n$  give the initial points of those trajectories that correspond to multipacting. A recomputation of the trajectories starting at the minima of  $d_n$  can be used to analyze the nature of the multipacting process. The important questions are the order of the multipacting (number of rf cycles per wall impact), whether it is a one-point or multi-point multipacting and whether it is due mostly to the magnetic or electric field.

Finally, the kinetic energy condition for each multipacting process has to be checked. If the impact energies are too low or too high, no multipacting will occur even if the geometric conditions are satisfied. The kinetic energy check was done by computing the number  $\alpha_n$  defined earlier for the potentially multipacting trajectories.

#### A. Coaxial cable: Scaling laws in SW operation

The multipacting analyzer was first applied to straight coaxial lines in standing wave (SW) operation. The computations were done in a half wavelength long section of the line.

The following is a summary of the results. First, the analysis showed that multipacting in SW coaxial line fields is due to the electric field only. In fact, the powers that yield multipacting can be found by computing the trajectories at the electric field maximum only. Second, both one-point multipacting (from outer conductor to itself) and two-point multipacting (from outer to inner conductor and back) may occur. We analyzed the multipacting in lines with different sizes, different rf frequencies and

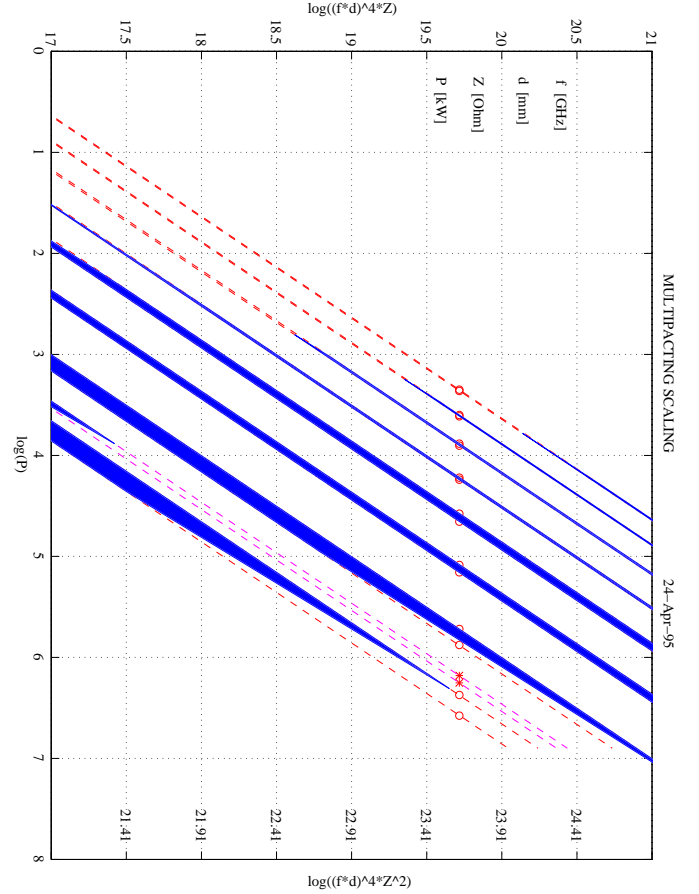


Figure 1. Multipacting bands in coaxial lines

different line impedances. It turned out that the multipacting powers obey quite accurately the following scaling laws:

$$P_{\text{one-point}} \sim (fd)^4 Z, \quad P_{\text{two-point}} \sim (fd)^4 Z^2,$$

where  $f$  is the rf frequency,  $d$  is a size parameter (in this paper  $d$  is the diameter of the outer conductor) and  $Z$  is the line impedance.

We computed the average impact energy of the electrons in multipacting trajectories. It was verified numerically that the average impact energy obeys roughly the scaling law

$$E_{\text{kin}} \sim (fd)^2,$$

in accordance to a simple dimension analysis. Typically the secondary electron yield for Niobium has a maximum around 400 eV, and is larger than one in the range  $\sim 100 - 1500$  eV.

Figure 1 is a graphical summary of the analysis. The upper horizontal axis is the natural logarithm of the number  $(fd)^4 Z$  (in  $(\text{GHz} \times \text{mm})^4 \times \text{Ohm}$ ). The one-point multipacting powers for a given coaxial line can be found by computing this number, drawing a vertical line and reading the powers where this line intersects the bands marked by circles. The lowest band is the first order one-point multipacting band. The next band upwards is a two-point first order band, then follows a set of one-point bands, the order increasing up to 8 when one moves up in the figure to lower powers. The kinetic energy condition  $100 \text{ eV} \leq E_{\text{kin}} \leq 1500 \text{ eV}$  when multipacting may occur is marked in

the picture by shading. Similarly, the lower horizontal axis is the logarithm of the number  $(df)^4 Z^2$  (in  $(\text{GHz} \times \text{mm})^4 \times \text{Ohm}^2$ ), characteristic for two-point multipacting. By computing this number and reading the intersection with the band marked with asterisks gives the multipacting powers. Note that there is only the first order two-point band in the picture; the higher order bands tend to get mixed with the more prominent two-point bands. Again, shading at the far left of the band indicates where the kinetic energy condition holds. With typical design parameters, the two-point process has a too large kinetic energy for multipacting. The circles and asterisks in the picture correspond to the 50 Ohm 1.3 GHz TESLA line.

### B. Transition to TW operation

It is important to understand the behavior of the multipacting levels when the field switches from standing wave to the traveling wave, i.e., the reflected wave vanishes. We repeated the computation with the coaxial line with no reflected wave, and found that the multipacting levels shift according to the simple rule

$$P_{TW} = 4P_{SW},$$

i.e., in the traveling wave operation each multipacting level appears at four times higher one-way rf power. There is a simple physical heuristic behind this phenomenon: The peak voltage in standing wave operation is twice the peak voltage of the traveling wave. The analysis of the trajectories show, however that the situation is a bit more subtle, since the multipacting electrons have to be traveling as the wave form moves.

### C. Other coaxial structures

The analysis algorithm has been applied so far to a set of coaxial structures. These include the tapered coaxial line and coaxial lines with an impedance step. Currently, we are running computations with grooved lines and certain ceramic window designs. The results will be reported in a forthcoming article.

### D. Test cavity

To test the method, we made computations in a geometry where direct multipacting measurements can be made. A test cavity with a direct access to the multipacting current as well as the experiment are described elsewhere in this proceedings ([2]). The electric field in the gap between the electrodes is fairly homogenous, and two-point multipacting of order  $n$  between the electrodes is expected at voltage drop close to

$$V_{(n)} = \frac{m_e}{e} \frac{4\pi f^2 d^2}{2n-1}. \quad (1)$$

This is the field giving resonant trajectories between two infinite parallel plates with time harmonic voltage drop. Figure 2 shows the counter function  $c_{30}$  versus the voltage between the electrodes on the symmetry axis. The two prominent bands correspond to the first and second order two-point multipacting between the electrodes. They agree well with the theoretical values (1), marked by an asterisk. The slight shift to the left is due to the positive initial velocity used in the trajectory calculations, not included in (1). This figure corresponds to the measured

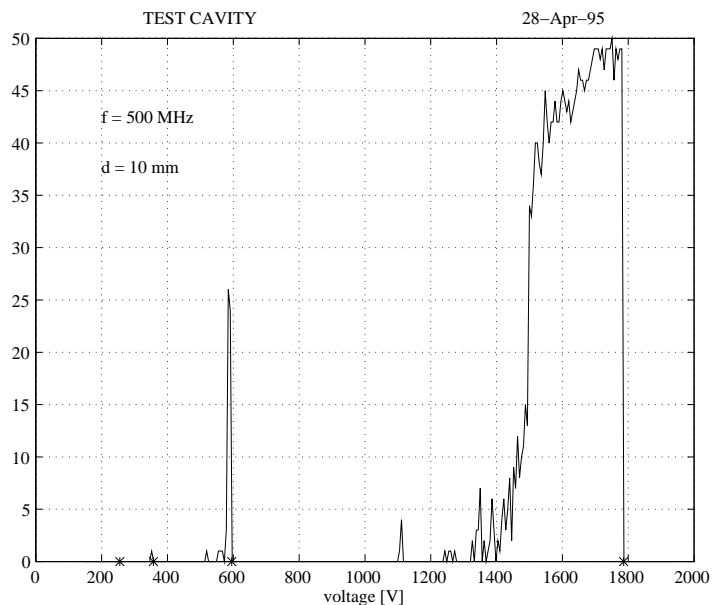


Figure 2. Multipacting counter function for the test cavity

curve in Figure 3 in [2]. Let us mention that the computed kinetic energy for the second order process is typically too low to appear with secondary electron yields characteristic e.g. to Niobium surfaces.

### References

- [1] E. Somersalo, P. Ylä-Oijala and D. Proch: Electron multipacting in RF structures. TESLA Reports 14–94.
- [2] D. Proch, D. Einfeld, R. Onken and N. Steinhauser: Measurement of multipacting currents of metal surfaces in RF fields. WPQ24 (This conference).